THE JOURNAL OF BIOLOGICAL CHEMISTRY
Vol. 280, No. 24, Issue of June 17, pp. 22582–22589, 2005

Printed in U.S.A.

NMR Analysis of Synthetic Human Serum Albumin α-Helix 28 Identifies Structural Distortion upon Amadori Modification*

Received for publication, February 8, 2005, and in revised form, March 31, 2005
Published, JBC Papers in Press, April 18, 2005, DOI 10.1074/jbc.M501480200

Mark J. Howard and C. Mark Smales‡

From the Protein Science Group, Department of Biosciences, University of Kent, Canterbury, Kent, CT2 7NJ, United Kingdom

The non-enzymatic reaction between reducing sugars and long-lived proteins *in vivo* results in the formation of glycation and advanced glycation end products, which alter the properties of proteins including charge, helicity, and their tendency to aggregate. Such protein modifications are linked with various pathologies associated with the general aging process such as Alzheimer disease and the long-term complications of diabetes. Although it has been suggested that glycation and advanced glycation end products altered protein structure and helicity, little structural data and information currently exist on whether or not glycation does indeed influence or change local protein secondary structure. We have addressed this problem using a model helical peptide system containing a di-lysine motif derived from human serum albumin. We have shown that, in the presence of 50 mM glucose and at 37 °C, one of the lysine residues in the di-lysine motif within this peptide is preferentially glycated. Using NMR analysis, we have confirmed that the synthetic peptide constituting this helix does indeed form a α-helix in solution in the presence of 30% trifluoroethanol. Glycation of the model peptide resulted in the distortion of the α-helix, forcing the region of the helix around the site of glycation to adopt a 3_{10} helical structure. This is the first reported evidence that glycation can influence or change local protein secondary structure. The implications and biological significance of such structural changes on protein function are discussed.

Non-enzymatic glycation describes the initial products arising from the formation of Maillard reaction adducts due to the reaction between primary amino groups on a protein surface and reducing sugars such as glucose and fructose (1–4). These non-enzymatic reactions are initiated with the reversible formation of a Schiff base adduct that undergoes rearrangement to form a more stable Amadori product (for glucose) (5) or Heyns product (for fructose) (6). The Amadori compound may then undergo a series of poorly understood rearrangements and reactions to yield protein adducts collectively termed advanced glycation end products (AGEs)[1] (4). AGEs are naturally formed *in vivo* on a variety of proteins and are implicated in the pathologies associated with aging, atherosclerosis, Alzheimer disease, and long-term diabetic complications (7). More recently, glycation has been shown at the N terminus of the pathogenic prion protein in transmissible spongiform encephalopathies, a group of transmissible neurodegenerative diseases that are characterized by the accumulation of abnormally folded prion protein (8), and has been implicated in food allergies (9).

The association of AGEs with a variety of pathologies has resulted in much scientific interest in the role played by glycation products and AGEs in the pathology of these disease states. For example, in recent years, the receptor for advanced glycation end products has been described and it has since been reported to be a member of the immunoglobulin superfamily of cell surface proteins (10). The expression of receptor for advanced glycation end products has also been implicated as a developmental factor in several pathologic conditions including chronic inflammation, cancer, and Alzheimer disease (10). Furthermore, a number of AGE products and cross-links have now been described (11); however, despite much attention, the exact role that these modified protein forms play in the associated disease states remains to be fully elucidated.

The process of glycation and the formation of AGEs are known to promote protein aggregation and insolubilization (12). Furthermore, protein glycation and the formation of subsequent AGE products are thought to be involved in structural and functional changes *in vivo* in proteins during aging and the long-term complications of diabetes (12, 13). Although glycation has been shown to inactivate a number of enzymes (12), little information, if any, currently exists regarding the effects these modifications have on protein secondary or tertiary structure. This is largely due to the problem of obtaining sufficient homogeneous material for structural studies, because glycation usually occurs at one or more residues on a protein structure and gives rise to multiple AGEs.

Notwithstanding these apparent problems, Blakytny *et al.* (12) used mass spectrometry and NMR to study the effect of glycation with galactose on the C-terminal extension of α-crystallin, investigating both the intact protein and a synthetic C-terminal peptide (12). Although these studies categorically identified the sites and level of glycation, both the intact protein and synthetic peptide exhibited great conformational freedom and adopted no preferred structure in solution and therefore no conclusions could be drawn regarding the effect of glycation on the secondary and tertiary structure of α-crystal-

* This work was supported by Grant BB/C504600/1 from the Biotechnology and Biological Sciences Research Council (BBSRC). The costs of publication of this article were defrayed in part by the payment of page charges. This article must therefore be hereby marked "*advertisement*" in accordance with 18 U.S.C. Section 1734 solely to indicate this fact.

‡ To whom correspondence should be addressed: Dept. of Biosciences, Protein Science Group, University of Kent, Canterbury, Kent, CT2 7NJ, United Kingdom. Tel.: 44-01227-823746; Fax: 44-01227-763912; E-mail: c.m.smales@kent.ac.uk.

[1] The abbreviations used are: AGEs, advanced glycation end products; HSA, human serum albumin; CD, circular dichroism; CNS, crystallography and NMR system; DQFCOSY, double-quantum filtered correlated spectroscopy; HPLC, high performance liquid chromatography; NMR, nuclear magnetic resonance; NOE, nuclear Overhauser effect; pBS, phosphate-buffered saline; NOESY, nuclear Overhauser effect spectroscopy; r.m.s., root mean square; ROESY, rotating frame Overhauser effect spectroscopy; TOCSY, total correlation spectroscopy.

lin (12). NMR has also been used recently to detect the presence of glycated protein in the saliva of patients with diabetes (14), whereas others (15) have used it to study the effect of glycation on a tetrapeptide and its N-terminal amide bond stereochemistry and tautomeric distribution.

Despite these studies, little information currently exists on whether or not glycation does indeed influence or change local protein secondary structure. A previous study (16) on human serum albumin suggests that glycation does indeed result in conformation change, although the nature of this change was undetermined. Others (11) have reported that glycation and AGE product formation alter the helicity of proteins. In the present study, we have addressed this problem using a model peptide system derived from human serum albumin (HSA). Human serum albumin (ExPASy primary accession number P02768) is a helical protein that is the main protein constituent of plasma. Although the exact function of HSA is unknown, its primary function is thought to be to regulate the colloidal osmotic pressure of blood (17). The primary site of glycation in human albumin, both *in vitro* and *in vivo*, is known to be Lys^{525} (16). However, several other lysine residues in albumin are known to be glycated both *in vitro* and *in vivo*, including Lys^{548} as shown in a study of bovine albumin (18). Furthermore, the lysine residue, Lys^{548}, resides in the same helix and in the same peptide motif in both human and bovine serum albumin. Lys^{548} is of particular interest, because it lies in a di-lysine motif (Lys^{548}-Lys^{549}) that is part of a helix on the surface of the molecule (helix 28), which is held in place relative to the rest of the molecule via a salt bridge. Furthermore, glycation is thought to be accelerated at di-lysine motifs due to local acid-base catalysis.

Therefore, the model peptide used in this study corresponds to helix 28 of HSA, corresponding to residue numbers 543–557 in accordance with Swiss-Prot numbering. We have shown that, in the presence of glucose, one of the lysine residues in the di-lysine motif (Lys^{548}-Lys^{549}) within this peptide is preferentially glycated. As in the intact protein, the lysine equating to Lys^{548} was preferentially glycated in the model peptide system. Furthermore, using NMR analysis, we have confirmed that the synthetic peptide constituting this helix (residues 543–557) does indeed form a α-helix in solution in the presence of 30% trifluoroethanol (TFE). Glycation of the model peptide resulted in the distortion of the α-helix, forcing the region of the helix around the site of glycation to adopt a 3_{10} helical structure. This is the first reported evidence that glycation can indeed influence or change local protein secondary structure. The implications for such changes on protein function are discussed.

EXPERIMENTAL PROCEDURES

Materials—All of the materials were of analytical reagent grade or better and were purchased from Sigma unless otherwise stated.

Synthesis and Purification of Peptide HSA543–557—The peptide RERQIKKQTALVELV was synthesized with an acetylated N-terminal amino group using a Shimadzu PSSM-8 multiple peptide synthesizer and an Fmoc (*N*-(9-fluorenyl)methoxycarbonyl)/HBTu (O-(1H-benzotriazole-1-yl)-*N*,*N*,*N*′,*N*′-tetramethyluronium tetrafluoroborate) synthesis strategy. The resulting peptide was then purified by reverse phase HPLC using a preparative C_{18} 10 × 250 mm column linked to a Hewlett Packard 1100 series HPLC. The sample to be analyzed was injected onto the column, and salts were washed out with an isocratic gradient of 2% acetonitrile containing 0.05% trifluoroacetic acid. The peptide was then eluted from the column using a linear gradient from 2 to 40% acetonitrile (containing 0.045% trifluoroacetic acid) over 50 min. The peptide peak was collected and then freeze-dried overnight. Multiple runs were combined to purify all of the synthesized peptide. The authenticity of the purified peptide was then confirmed by mass spectrometry. Mass spectra were recorded in the positive ion mode using the extended mass range (*m/z* 250–4000) on a Finnigan MAT LCQ ion-trap mass spectrometer.

Generation and Isolation of Glycated Peptide HSA543–557—To generate glycated peptide, the peptide was dissolved in sterile PBS containing 50 mM glucose at a concentration of 5 mg/ml. The resulting solution was then incubated at 37 °C for 1 week. Prior to further experiments, salts and sugar components were then removed from the peptide solution by reverse phase HPLC as described above. Glycated peptide was then isolated from non-glycated peptide for NMR and mass spectrometric analysis using commercially available Glyco Gel™ columns (1-ml bed volume) from Pierce (Rockford, IL). The incubated peptide sample from which the salt/sugar components had been removed previously by reverse phase chromatography was then redissolved in 0.05 M HEPES (pH 8.5) and loaded onto the columns preequilibrated in the equilibration/wash buffer provided by Pierce. The column was then washed (5-column volumes), and the glycated peptide was eluted (in 3-column volumes) using the procedure previously described by Zhao *et al.* (19). The glycated fraction was then desalted by reverse phase chromatography, as described above, and freeze-dried. Control, non-glycated peptide for NMR analysis was generated by heating the synthesized and purified peptide at 5 mg/ml for 1 week at 37 °C in PBS (*i.e.* in the absence of glucose), desalted by reverse phase HPLC, and freeze dried. Both the glycated and non-glycated HSA543–557 peptides were then subjected to electrospray mass spectrometry (as described above) and NMR analysis.

NMR Sample Preparation—All of the NMR samples were prepared to a final volume of 300 μl for use in a Shigemi BMS005V NMR tube by dissolving purified, freeze-dried peptide to provide a final concentration of 2 mM peptide in PBS at pH 6.4 (phosphate concentration 25 mM and saline concentration of 100 mM). To this system, TFE-d_3 was added as a helix stabilizer to provide a final concentration of 30% (v/v) in the system. TFE was used following AGADIR (20, 21) analysis of the peptide that identified the helical propensity of the standard peptide as 0.21. Peptides with this level of propensity will only highlight regions of helical tendency with the addition of TFE (20). 30% (v/v) TFE was considered the lowest proportion of TFE that could be used to give rise to a helical structure. This was confirmed from the NMR NOE contacts observed for the standard helix. To make a meaningful comparison, all of the Amadori modified peptide data were obtained under identical conditions to those used for the standard peptide.

NMR Spectroscopy—All of the experiments were recorded at 10 °C on a Varian UnityINOVA 600 MHz NMR spectrometer with a *z*-shielded gradient triple resonance probe using standard procedures. For each peptide sample, a two-dimensional nuclear Overhauser effect spectroscopy (NOESY) and total correlation spectroscopy (TOCSY) experiments were recorded with mixing times of 250 and 68.4 ms, respectively. These experiments were collected with 512 and 1024 complex points with acquisition times of 64 and 128 ms in the indirectly and directly acquired ^{1}H dimensions, respectively. The maximum theoretical NOESY enhancement was estimated to be between 70 and 90% theoretical maximum, whereas our projected ROESY enhancements were expected to be 60%. Therefore, NOESY experiments were chosen in this analysis and validated by obtaining build-up curves that also confirmed 250 ms as the most appropriate mixing time. In addition, a two-dimensional double-quantum-filtered correlated spectroscopy (DQFCOSY) experiment was collected for each peptide with 1024 and 2048 complex points with acquisition times of 128 and 256 ms in the indirectly and directly acquired ^{1}H dimensions, respectively. Amides in slow exchange and deemed capable of being hydrogen bond donors were identified from a NOESY experiment that was collected with 256 and 1024 complex points with acquisition times of 32 and 128 ms in the indirectly and directly acquired ^{1}H dimensions, respectively, obtained from a peptide sample resuspended in ^2H_2O. Data processing and analysis were carried out on Sun Blade 100 and Transtec X2100 Linux workstations using NMRPipe (22) to process and NMRView (23) to view processed data.

Structural Calculations and Analysis—All of the structural calculations were obtained using the Crystallography and NMR System (CNS), version 1.1 (25, 38), running on Silicon Graphics O_2+ and Transtec X2100 Linux workstations. CNS parameter files were modified to incorporate the topology of the modified lysine residue for calculations. All of the NOE contacts were classified into one wide classification between 1.8 and 5.0 Å with final structures calculated from extended coordinates using the standard CNS NMR anneal protocol with the sum averaging for dynamic annealing with NOEs from both extended and folded precursors (24). A final structural ensemble of 40 structures for each peptide was produced with all of the structures used to produce statistical energy and root mean square (r.m.s.) deviation structural information. Backbone and heavy atom r.m.s. deviation values were obtained using MOLMOL, version 2k.2 (25), on a computer running Microsoft Windows 2000. The structural integrity of each ensemble was evaluated using PROCHECK-NMR (26) run on a Transtec X2100 Linux workstation. Energy comparisons between structures created from the

TABLE I
Mass spectral characterization data of the unmodified and glycated HSA543–557 synthetic peptide

Peptide	Theoretical $[M+H]^{+a}$	Measured $[M+H]^{+a}$	Theoretical $[M+2H]^{2+a}$	Measured $[M+2H]^{2+a}$
Unmodified	1853.1	1853.2	927.1	927.5
Glycated	2015.1	2015.2	1008.1	1008.2

[a] Monoisotopic mass.

NMR constraint data and the equivalent human serum albumin helix were made using GROMOS96 43Bl parameter set (27) within DEEPVIEW, version 3.7 (28).

RESULTS

Peptide Synthesis, Glycation, and Purification—The peptide sequence corresponding to HSA α-helix 28 (residues 543–557) was successfully synthesized on a Shimadzu PSSM-8 multiple peptide synthesizer as determined by mass spectrometry (Table I). The peptide sequence was identical to that found in the native HSA molecule with the exception that the N-terminal lysine residue was replaced with an arginine residue to prevent glycation on the lysine amino side chain of this residue (Lys^{543}). The peptide was synthesized with the N-terminal amino group blocked with an acetyl group to prevent potential glycation at this site in the synthetic peptide. Following incubation with glucose and purification of the glycated peptide from non-glycated peptide using a Glyco Gel column, mass spectrometry analysis confirmed that the peptide was glycated with one glucose residue per peptide molecule (*i.e.* not di-glycated), as indicated by an increase in the $[M+H]^+$ ion by 162 Da (Table I). From these data, it was not possible to confirm whether glycation had occurred entirely at one lysine residue, preferentially at one of the two-lysine residues in the di-lysine motif, or whether there was an equal distribution between the two. This was resolved during the NMR analysis (see below). We note that it has previously been shown that the sugar moieties in glycated human serum albumin occur as an equilibrium of the β-pyranose (59%), α-furanose (19%), and β-furanose (24%) anomers (29). Phenylboronate purification of Amadori products selectively binds β-furanose sugar anomers; however, because the confirmations are in rapid equilibrium, the yield of glycated peptide is likely to be close to quantitative.

NMR Resonance Assignments—Spin systems were identified by analysis of two-dimensional DQFCOSY and TOCSY NMR spectra, and all of the observed ^1H chemical shifts are listed in Table II. Assignments for the majority of ^1H spin systems were possible for both the standard and Amadori-modified peptide with the exception of amino acid Ile^{547} in the standard peptide. The H^α shift of the N-terminal amino acid Arg^{543} was not observed in either standard or modified peptide. The assignment of the modified Amadori lysine was possible following the observation of a duplicated set of resonances in the H^N region of the TOCSY spectrum for the modified lysine side chain (H^β, H^γ, H^δ, and H^ϵ). The first set of resonances are correlated from the backbone H^N of the lysine, but chemical modification transforms the side chain lysine NH_3^+ group to a H^N group (H^ζ) and provides a second H^N correlation and duplication of the lysine side chain ^1H resonances. Resonances of the Amadori peptide were achieved from both the DQFCOSY and TOCSY data together with H^η protons identified by the NOESY through-space correlation to H^ζ.

Structural Assignments and Additional Restraints—Through-space assignments were achieved using two-dimensional NOESY spectra of both standard and Amadori-modified peptide (see Fig. 1). Amides in slow exchange and deemed capable of being hydrogen bond donors were identified from a NOESY experiment obtained from a peptide sample resuspended in ^2H_2O. Additional ϕ restraints were obtained from the application of the Karplus relationship to $^3J_{HNH\alpha}$ that were obtained from high resolution DQFCOSY spectra. $^3J_{HNH\alpha}$ values <5 Hz were used to constrain ϕ for that residue to $-60 \pm 30°$. A cut-off value of 5 Hz was used to allow for the fact that $^3J_{HNH\alpha}$ values obtained by DQFCOSY are always larger than those obtained by more accurate heteronuclear NMR methods (30).

With the exception of Ile^{547} in the standard peptide where an NOE distribution was not observed, the NOE distribution was uniform across all of the residues in both peptides. A total of 23 NOEs were found between the modified Lys^{548} and residues Arg^{545}, Gln^{546}, and Ile^{547} that were crucial in defining the structural changes upon modification. A summary of the number of contact types and additional restraints are shown in Table III with the distribution of restraints across each peptide shown in Fig. 2, *a* and *b*. NOE contact types observed in Fig. 2*a* for the standard peptide support a standard helix conformation with NOEs observed between H^α:i and H^N:$i + 3$ as well as H^α:i and H^β:$i + 3$. Additionally, slow H^N exchange and $^3J_{HNH\alpha}$ values <5 Hz were observed for the majority of residues within the standard peptide with the exception of Ile^{547}, as the resonances from this residue were not observed in our system. The resonances from Ile^{547} were difficult to assign because of placement of the H^α resonance directly over the water resonance. This was confirmed by observing and assigning Ile^{547} resonances in the absence of TFE (data not shown). Fig. 2*b* highlights the NOE contact types for the Amadori-modified peptide and defines a region from Lys^{549} to Glu^{555} that shows similar helix NOE contacts to those observed throughout the standard peptide. This is also confirmed from the observed H^N exchange and $^3J_{HNH\alpha}$ values obtained for the modified peptide. The N-terminal region of the Amadori peptide gave rise to reduced H^α:i and H^N:$i + 3$ but increased H^α:i and H^β:$i + 3$ together with H^α:i and H^N:$i + 2$ and $i + 3$ contacts. In this region, there was a single retarded H^N exchange and no $^3J_{HNH\alpha}$ values <5 Hz.

Structure Calculations and Analysis—All of the structural data were determined using CNS as described under "Experimental procedures." No calculated structure gave violations greater than 0.2 Å or bond angle violations greater than 5° from the restraint data when all 40 structures were used to compute the ensemble average structural set. R.m.s. deviation statistics over all backbone atoms for residues 544–556 for the ensemble of 40 structures for both the standard and Amadori-modified peptide were found to be 0.37 and 0.48 Å, respectively. The backbone ensembles for both peptides are shown in Fig. 3, *a* and *b*, respectively, together with the ensemble average structures and key residues shown as ribbon schematics in Fig. 3, *c–f*. Corresponding r.m.s. deviations over all of the heavy atoms for each 40-structure ensemble of the standard and Amadori-modified peptides were found to be 1.29 and 1.45 Å, respectively. PROCHECK-NMR analysis of the Ramachandran plot for the 40-structure ensemble of the standard peptide identified that 100% of all of the residues fell in either the most favored or additionally allowed regions of the α-helix. Equivalent analysis of the Amadori-modified peptide identified 84.6% of all of the residues falling in the most favored or additionally allowed regions with the remaining 15.4% falling into the generously allowed regions of the α-helix. Ensemble average energies for each peptide are shown in Table IV together with the equivalent energies created from helix 28 extracted directly from the HSA x-ray structure.

TABLE II

NMR assignment list of observed ^1H chemical shifts for the standard and Amadori-modified peptide in PBS, 30% (v/v) TFE at 10 °C

All of the chemical shifts are referenced externally to 100 μM solution of dimethylsilapetane sulfonic acid in PBS, 30% (v/v) TFE.

Residue	H^N	H^α	Others
Standard Peptide			
Arg^{543}			$H^{\beta2/\beta3}$ 1.703; $H^{\gamma2/\gamma3}$ 1.845; $H^{\delta2/\delta3}$ 3.220
Glu^{544}	8.485	4.385	$H^{\beta2/\beta3}$ 2.132; $H^{\gamma2/\gamma3}$ 2.440
Arg^{545}	8.261	4.235	$H^{\beta2/\beta3}$ 1.843; $H^{\gamma2/\gamma3}$ 1.682; $H^{\delta2/\delta3}$ 3.222
Gln^{546}	8.981	4.182	$H^{\beta2/\beta3}$ 2.04; $H^{\gamma2/\gamma3}$ 2.315; $H^{\epsilon21/\epsilon22}$ 6.879/7.624
Ile^{547}			
Lys^{548}	8.516	4.160	$H^{\beta2/\beta3}$ 1.685, 1.828; $H^{\gamma2/\gamma3}$ 1.438/1.516; $H^{\delta2/\delta3}$ 1.700/1.858; $H^{\epsilon2/\epsilon3}$ 2.988
Lys^{549}	8.205	4.412	$H^{\beta2/\beta3}$ 1.663/1.865; $H^{\gamma2/\gamma3}$ 1.901; $H^{\delta2/\delta3}$ 1.706; $H^{\epsilon2/\epsilon3}$ 3.279
Gln^{550}	8.416	4.306	$H^{\beta2/\beta3}$ 2.118; $H^{\gamma2/\gamma3}$ 2.416; $H^{\epsilon21/\epsilon22}$ 6.823/7.512
Thr^{551}	8.129	4.269	H^{β} 4.238; $H^{\gamma2}$ 1.229
Ala^{552}	8.139	4.333	H^{β} 1.446
Leu^{553}	8.069	4.310	$H^{\beta2/\beta3}$ 1.616; H^{γ} 1.677; $H^{\delta1/\delta2}$ 0.888/0.944
Val^{554}	7.833	4.098	H^{β} 2.121; $H^{\gamma1/\gamma2}$ 0.961
Glu^{555}	8.275	4.322	$H^{\beta2/\beta3}$ 1.957/2.086; $H^{\gamma2/\gamma3}$ 2.320
Leu^{556}	8.154	4.416	$H^{\beta2/\beta3}$ 1.708; H^{γ} 1.627; $H^{\delta1/\delta2}$ 0.889/0.943
Val^{557}	7.518		H^{β} 2.109; $H^{\gamma1/\gamma2}$ 0.913
Amadori peptide			
Arg^{543}			$H^{\beta2/\beta3}$ 1.681/1.753; $H^{\gamma2/\gamma3}$ 1.869; $H^{\delta2/\delta3}$ 3.246
Glu^{544}	9.062	4.145	$H^{\beta2/\beta3}$ 2.094; $H^{\gamma2/\gamma3}$ 2.380
Arg^{545}	7.383	4.215	$H^{\beta2/\beta3}$ 1.686, 1.764; $H^{\gamma2/\gamma3}$ 1.924; $H^{\delta2/\delta3}$ 3.285
Gln^{546}	8.411	4.269	$H^{\beta2/\beta3}$ 2.190, 2.190; $H^{\gamma2/\gamma3}$ 2.480; $H^{\epsilon21/\epsilon22}$ 6.784/7.413
Ile^{547}	8.118	3.991	H^{β} 1.474; $H^{\gamma2}$ 1.217; $H^{\gamma12/\gamma13}$ 0.946; $H^{\delta1}$ 0.886
Lys^{*548}	8.275	4.213	$H^{\beta2/\beta3}$ 1.587, 1.931; $H^{\gamma2/\gamma3}$ 1.473; $H^{\delta2/\delta3}$ 1.772; $H^{\epsilon2/\epsilon3}$ 3.260; H^{ζ} 8.556; $H^{\eta2/\eta3}$ 3.260/4.173; $H^{\iota2}$ 4.678; $H^{\kappa2}$ 3.290; $H^{\lambda2}$ 3.480; $H^{\mu2/\mu3}$ 3.444/3.528
Lys^{549}	8.039	4.193	$H^{\beta2/\beta3}$ 1.923; $H^{\gamma2/\gamma3}$ 1.678, 1.772; $H^{\delta2/\delta3}$ 1.772; $H^{\epsilon2/\epsilon3}$ 3.283
Gln^{550}	8.042	4.257	$H^{\beta2/\beta3}$ 2.181; $H^{\gamma2/\gamma3}$ 2.435; $H^{\epsilon21/\epsilon22}$ 6.840/7.558
Thr^{551}	8.148	4.323	H^{β} 4.244; $H^{\gamma2}$ 1.281
Ala^{552}	8.054	4.325	H^{β} 1.502
Leu^{553}	8.012	4.305	$H^{\beta2/\beta3}$ 1.790; H^{γ} 1.656; $H^{\delta1/\delta2}$ 0.945
Val^{554}	7.778	4.089	H^{β} 2.201; $H^{\gamma1/\gamma2}$ 1.018
Glu^{555}	8.114	4.383	$H^{\beta2/\beta3}$ 2.058/2.168; $H^{\gamma2/\gamma3}$ 2.388/2.470
Leu^{556}	8.078	4.450	$H^{\beta2/\beta3}$ 1.688/1.790; H^{γ} 1.764; $H^{\delta1/\delta2}$ 0.913/0.960
Val^{557}	7.531	4.123	H^{β} 2.166; $H^{\gamma1/\gamma2}$ 0.963

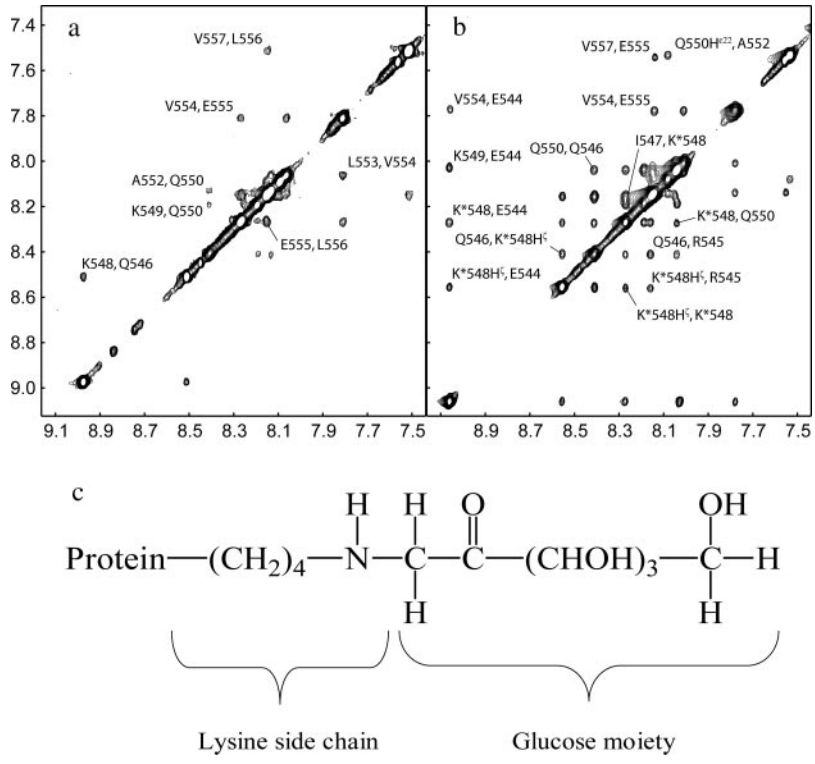

FIG. 1. Fingerprint H^N-H^N region of two-dimensional NOESY NMR spectra for standard (*a*) and Amadori-modified (*b*) peptides obtained using 250-ms mixing periods is shown. All of the assignments are illustrated in the format [vertical (F1) ppm, horizontal (F2) ppm] and are for H^N unless stated. *c*, the chemical structure of the glycated lysine residue.

DISCUSSION

Incubation of the model HSA peptide in glucose resulted in the glycation of Lys^{548}, as determined by NMR spectroscopy (see below), in preference to Lys^{549}. Although Lys-Lys sequences are known to be more reactive toward protein glycation due to local acid-base catalysis, it is also thought that preferential protein glycation at one lysine residue in a di-lysine motif is, at least partially, due to the relative accessibilities of the two lysine side chains in question (2, 31). However, the model peptide used in this study exhibited no measurable secondary structure in aqueous PBS solution in the absence of TFE and therefore stabilized structural aspects would not ap-

TABLE III
List of NOE, hydrogen bond, and torsion angle connectivities for both standard and Amadori-modified peptide

		Standard peptide	Amadori-modified peptide
NOEs	Intraresidue	32	36
	Sequential	74	61
	$i - i + 2$	28	24
	$i - i + 3$	76	75
	$i - j$ (>3)	22	30
	Total	232	226
Retarded amide hydrogen exchange		9	5
Tortion angles	ϕ	8	5

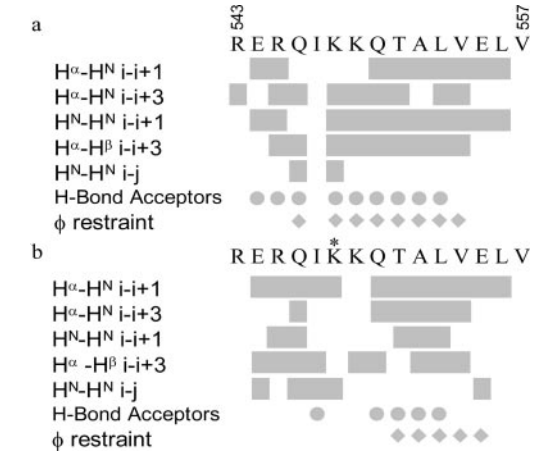

FIG. 2. **Schematic of NOE contact types, hydrogen bond acceptors, and residues giving rise to ϕ restraints for both the standard (*a*) and Amadori-modified (*b*) peptides.**

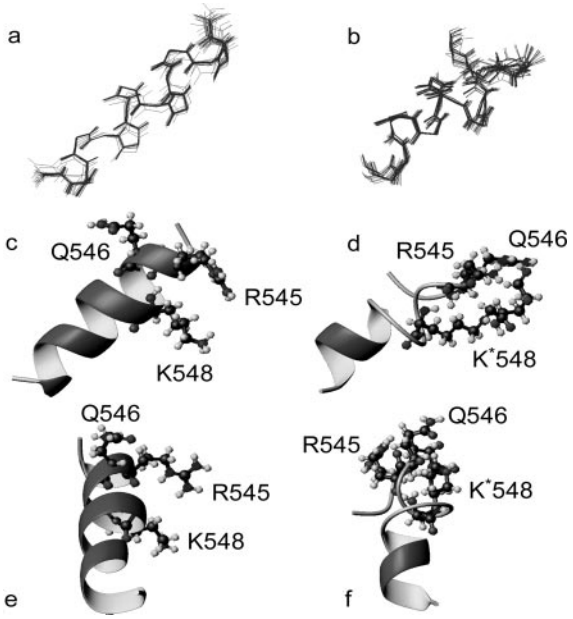

FIG. 3. Superimposition of all backbone bonds of the 40-structure ensemble calculated from NMR data for standard peptide (*a*) and Amadori-modified peptide (*b*) is shown. *c–f*, ribbon diagrams created in MOLMOL of the ensemble average structures are shown of the standard peptide (*c* and *e*) and Amadori-modified peptide (*d* and *f*). Key residue side chains are labeled and shown as ball and stick structures. *e* and *f* were created by 90° anti-clockwise rotation through a vertical axis defined in *c* and *d*. *d* clearly shows the site of the carbohydrate moiety attached to Lys^{548}.

pear to account for the exclusive glycation of Lys^{548} in preference to Lys^{549}. Preferential glycation at Lys^{548} could be due to local acid-base catalysis and the immediate neighboring amino acids, resulting in the amino group of Lys^{548} being more nucleophilic than that of Lys^{549}; however, it is clear that long-range structural affects must be involved because the adjacent Ile^{547} is unlikely to affect the pK_a of Lys^{548}. We suggest that it is possible that, although the mean structure is random in aqueous PBS solution, the chemical modification of Lys^{548} is catalyzed when the random coil approximates the helical structure in the protein. This may occur when the side chain of Arg^{545} approaches that of Lys^{548} and the charge on Arg^{545} suppresses the charge on (and lowers the pK_a of) Lys^{548}. However, it is also likely that Glu^{544} may be in a position to catalyze the Amadori rearrangement on Lys^{548}. In this respect, it is interesting that the position of Glu^{544} is significantly altered in the glycated peptide relative to the non-glycated (standard) peptide (see Fig. 4).

TABLE IV
Average ensemble energies (kJ mol^{-1}) for calculated structures of both standard and Amadori-modified peptide obtained from DEEPVIEW using GROMOS96

Energies for the equivalent helix within HSA structure 1AO6.pdb are also shown for comparison.

Energy	Standard	Amadori	Helix from HSA 1AO6.pdb
Bonds	15.09	15.98	10.70
Angles	66.78	97.60	65.10
Torsions	78.01	45.40	76.20
Impropers	23.43	30.20	20.90
Nonbonded	−246.76	−269.73	−366.79
Electrostatic	−697.03	−526.09	−454.85
Total (kJ mol^{-1})	−760.48	−606.64	−648.74

The H^{α} chemical shift differences between the standard and modified peptide were found to be moderately small with the exception of residues Glu^{544} and Lys^{549} as indicated in Fig. 4. This finding suggests that similar local conformation exists across the entirety of both peptides in accordance with known observations of H^{α} chemical shift in the prediction of secondary structure elements (32). Upon initial inspection, one may be lead to believe that Lys^{549} is the modified peptide on the basis of the H^{α} shift difference alone because of the large difference in H^{α} chemical shift. We know from both NOESY and chemical shift assignments, as outlined under "Results," that Lys^{548} is modified in the glycated peptide. This is also confirmed by analysis of the H^{ϵ} chemical shift values for Lys^{548} and Lys^{549} in both the standard and modified peptide. The ^1H chemical shift difference between the standard and modified peptide for Lys^{548} H^{ϵ} is 0.272 ppm compared with 0.058 ppm observed for Lys^{549}. Because the H^{ϵ} is in close proximity to the modification, it stands to reason that the greatest shift change will be observed by the H^{ϵ} of the lysine that is modified, in this case, Lys^{548}.

The standard peptide in 30% (v/v) TFE folds to form an α-helical peptide structure (Fig. 3). All of the NOE contact data, hydrogen exchange, and $^3J_{HNH\alpha}$ data support this observation, and the ensemble of 40 structures provides a model whereby 100% modeled amino acids in the ensemble fall inside the allowed regions for an α-helix in a Ramachandran plot. Fig. 3, *c* and *e*, shows a ribbon form of the ensemble average structure that adopts a helix with key residues Arg^{545} and Lys^{548} on one

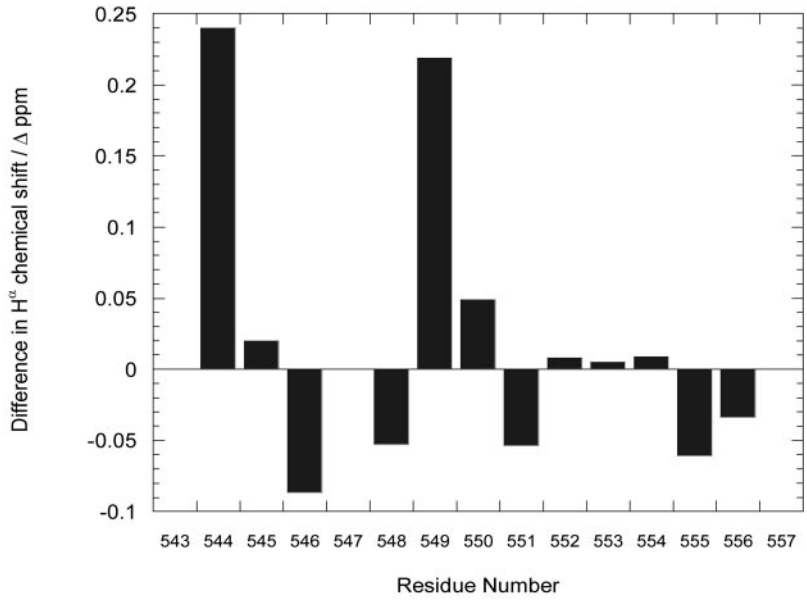

FIG. 4. **Difference in $^1H^{\alpha}$ NMR chemical shift observed for each residue in the standard and Amadori-modified peptide.**

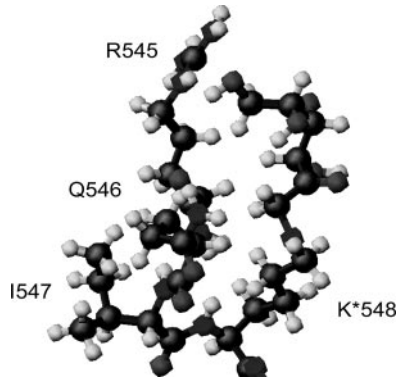

FIG. 5. **Ball and stick detail of interacting side chains Arg^{545}, Gln^{546}, Ile^{567}, and the modified lysine, Lys^{*548}, in the Amadori-modified peptide.**

face of the helix and Gln^{546} rotated on the top face of the peptide. The ribbon view highlights an exaggerated tightening of the helix at both the N and C termini that is most probably due to the CNS modeling. Because both terminal regions have no additional constraints from hydrogen bonding to assist in the calculation and modeling of the peptide helical structure, these regions will tend to tighten slightly as observed within the calculation. Narrower helical ϕ angle constraints could have been used at the termini to reduce this effect, but it was considered important not to over-constrain any aspect of the data and risk providing structural effects that could not be explained.

NMR data of the Amadori-modified peptide in 30% (v/v) TFE define a fold that forms a more complicated structure compared with the standard peptide. Figs. 2*b* and 3, *b*, *d*, and *f*, show the C-terminal region of the peptide from Gln^{550}-Thr^{551} toward the C terminus forming a standard helix that does not differ greatly from the standard peptide helix in this region. This is illustrated by the fact that the backbone r.m.s. deviation for residues Gln^{550} and Leu^{556} for an 80-structure ensemble (40 standard structures and 40 Amadori-modified structures) is only 0.25 Å. As with the standard peptide, the NOE contact data, hydrogen exchange, and $^3J_{HNH\alpha}$ data support the conclusion that the region from Gln^{550} to Leu^{556} is helical.

Fig. 5 shows the detailed arrangement of Arg^{545}, Gln^{546}, Ile^{547}, and the modified lysine, Lys^{*548}, in the Amadori-modified peptide in the ensemble average model that is supported

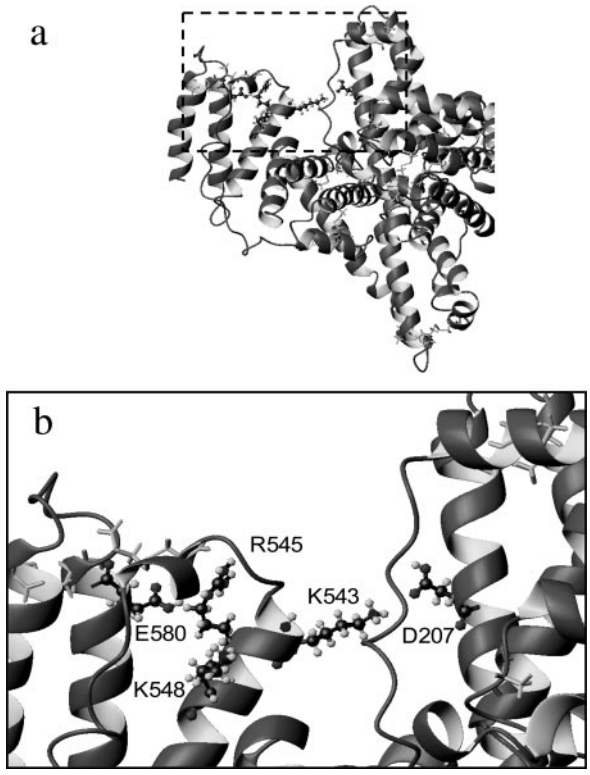

FIG. 6. ***a* and *b*, ribbon diagram of HSA showing the N-terminal region of helix 28 and adjacent electrostatic contact via Lys^{543} to Asp^{207} in helix 10.**

by 23 NOE interactions between residues 545–547 and the modified Lys^{*548}. Ile^{547} H^N and H^{α} have contacts to Lys^{*548} H^N, H^{α}, and H^{β}. Gln^{546} has NOE contacts from its side chain atoms $H^{\beta}$and H^{γ} to Lys^{*548} H^{β}, H^{γ}, H^{δ}, and H^{ϵ} as well as the modification protons H^{ζ} and H^{η}. Arg^{545} has NOE contacts from its side chain atoms H^{β}, H^{γ}, and H^{δ} to protons H^{ι}, H^{κ}, H^{λ}, and H^{μ} in the Amadori structure that can be seen clearly associated as a contact core in Fig. 5. This overall appearance is observed in all 40 structures of the ensemble with the modified carbohydrate chain on the lysine parallel to the side chain of Arg^{545}. This is confirmed in a quantitative manner by calculation of an r.m.s. deviation of 0.36 Å for all of the side chain carbon atoms from both Arg^{545} and Lys^{*548} over the 40-structure ensemble of

the modified peptide. It is likely that the interaction is stabilized by hydrogen bonding between protons on the Arg^{545} H^{ϵ} groups and hydroxyl oxygen atoms attached to Cμ of the modified Lys^{*548}. This arrangement would also be stabilized by an electrostatic attraction between Arg^{545} side chain $NH_{2\epsilon}$ groups and electronegative oxygen atoms attached to both Cμ and Cλ atoms in the modification. This association and contact between the modified glycated chain on Lys^{*548} and Arg^{545} twists the C-terminal region of the helix that is observed in the standard peptide. Interestingly, there still appears to be some helical character to this region as seen from the presence of H^{α}:*i* and H^{β}:*i* + 3 NOE contacts, which in this region appear more prevalent than H^{N}:*i* and H^{α}:*i* + 3 contacts. This finding suggests that this region adopts a conformation more in line with a 3_{10} helix as H^{α}:*i* and H^{β}:*i* to H^{N}:*i* + 2/:*i* + 3 are stronger in such systems (33).

Despite the suggestion of the model that the Amadori modification places structural strain on the peptide, PROCHECK analysis for the ensemble of 40 structures showed that 84.6% of the modeled amino acids resided inside the favored allowed regions for α-helix in a Ramachandran plot. It would appear that there is strain in ϕ/ψ for Gln^{546} and Ile^{547} and that this is created by the interaction of the Amadori Lys^{*548} side chain with Arg^{545} because the 15.4% that fell inside generously allowed regions consisted entirely of ϕ/ψ distributions from Gln^{546} and Ile^{547}. These two residues (Gln^{546} and Ile^{547}), together with Arg^{545}, provided virtually all of interactions with the modified Lys^{548} Amadori side chain.

An analysis of the Protein Data Bank coordinates for HSA shows that, in the intact protein structure, two disulfide bonds exist between Cys^{538}-Cys^{583} and Cys^{582}-Cys^{591} that hold helices 28, 29, and 30 together. This stabilization is further supported by an electrostatic attraction between the side chains of Arg^{545} and Glu^{580}. However, unlike much of the HSA structure, helices 28–30 at the C terminus are not attached to the bulk of the protein by a disulfide bond (only to each other) but are held relative to the bulk structure via a salt bridge created between the side chains of Lys^{543} of helix 28 and Asp^{207} in helix 10. This salt-bridge arrangement is depicted in Fig. 6. Close analysis of the modified structures shown in Fig. 3, *e* and *f*, confirmed an anticlockwise 90° twist in the orientation of the N terminus of the peptide upon modification that would remove the correct orientation of Lys^{543} with respect to its salt bridge with Asp^{207} in the intact protein. If disruption of this salt bridge was to occur in the intact protein, this would result in helices 28–30 becoming more flexible and mobile, loosening the protein structure, exposing hydrophobic residues, and increasing the susceptibility of the three helices to hydrolysis and cleavage from the structure. The reorientation of residues 543–548 would also remove the electrostatic interaction between Glu^{580} and Arg^{545} and destabilize the turn regions of helices 28–30. Previous NMR investigations on proteins with disulfide bonds have shown degrees of conformational flexibility around these bonds (34, 35), and any loss of nearby electrostatic stabilization will increase the conformational flexibility in the region around the disulfide bond, in this case around Cys^{538} and Cys^{583}. This would further destabilize the structure in this region of HSA.

We have clearly shown that glycation of a model peptide system can result in disruption of local secondary structure and alter helicity as suggested by Sell and Monnier (11). To our knowledge, this is the first example that definitively shows that glycation can influence and change secondary structural elements. Although we have not determined this change in helical structure in the intact HSA protein molecule upon glycation of Lys^{548}, we predict that the few interactions holding this part of the molecule together are likely to be disrupted by such a modification. This prediction disagrees with a previous study by Coussons *et al.* (36) who concluded that glycation had minimal effects on the folded structure of HSA; however, this observation was based on far-UV circular dichroism (CD) measurements, which will only detect gross changes in the secondary structure. The disruptions described and predicted here are unlikely to have been detected by far-UV CD. Furthermore, helix 28 is in the region of drug-binding site 2 in HSA and previous investigations have suggested that modification with methylglyoxal of an arginine residue in close proximity to Ile^{547} modifies the ligand binding and enzymatic activity of HSA domain 3A (37). Therefore, we suggest that glycation of Lys^{548} is also likely to change the ligand binding and enzymatic activity of this domain of HSA.

A similar disruption of secondary structure in other proteins could potentially affect protein function by, for example, changing enzymic activity, binding affinities, or exposing hydrophobic patches leading to protein aggregation. In this way, protein glycation and the formation of an Amadori product may be involved in accelerating protein aggregation even before the formation of AGE cross-links, which accumulate much more slowly. As such, the formation of an Amadori product alone could be envisaged as playing a role in pathologies such as those seen in transmissible neurodegenerative diseases characterized by the accumulation of an abnormally folded prion protein whereby post-translational glycation is known to occur (8).

Acknowledgments—We thank Judy Hardy and Kevin Howland for synthesizing the peptides used in this study.

REFERENCES

1. Lapolla, A., Fedele, D., Plebani, M., Aronica, R., Garbeglio, M., Seraglia, R., Dalpaos, M., and Traldi, P. (1999) *Clin. Chem.* **45,** 288–290
2. Smales, C. M., Pepper, D. S., and James, D. C. (2002) *Biotechnol. Bioeng.* **77,** 37–48
3. Smales, C. M., Pepper, D. S., and James, D. C. (2000) *Biotechnol. Appl. Biochem.* **32,** 109–119
4. Alikhani, Z., Alikhani, M., Boyd, C., Nagao, K., Trackman, P. C., and Graves, D. T. (2005) *J. Biol. Chem.* **280,** 12087–12095
5. Bucala, R. (1996) *Diagn. Endocrin. Metab.* **14,** 99–106
6. Suarez, G., Rajaram, R., Oronsky, A. L., and Gawinowicz, M. A. (1989) *J. Biol. Chem.* **264,** 3674–3679
7. Biemel, K. M., Friedl, D. A., and Lederer, M. O. (2002) *J. Biol. Chem.* **277,** 24907–24915
8. Choi, Y.-G., Kim, J.-I., Jeon, Y.-C., Park, S.-J., Choi, E.-K., Rubenstein, R., Kascsak, R. J., Carp, R. I., and Kim, Y.-S. (2004) *J. Biol. Chem.* **279,** 30402–30409
9. Davis, P. J., Smales, C. M., and James, D. C. (2001) *Allergy* **56,** 56–60
10. Hanford, L. E., Enghild, J. J., Valnickova, Z., Petersen, S. V., Schaefer, L. M., Schaefer, T. M., Reinhart, T. A., and Oury, T. D. (2004) *J. Biol. Chem.* **279,** 50019–50024
11. Sell, D. R., and Monnier, V. M. (2004) *J. Biol. Chem.* **279,** 54173–54184
12. Blakytny, R., Carver, J. A., Harding, J. J., Kilby, G. W., and Sheil, M. M. (1997) *Biochim. Biophys. Acta* **1343,** 299–315
13. Neglia, C., Cohen, H., Garber, A., Thorpe, S., and Baynes, J. (1985) *J. Biol. Chem.* **260,** 5406–5410
14. Yoon, M. S., Jankowski, V., Montag, S., Zidek, W., Henning, L., Schluter, H., Tepel, M., and Jankowski, J. (2004) *Biochem. Biophys. Res. Commun.* **323,** 377–381
15. Zigrovic, I., Kidric, J., and Horvat, S. (1998) *Glycoconj. J.* **15,** 563–570
16. Shaklai, N., Garlick, R., and Bunn, H. (1984) *J. Biol. Chem.* **259,** 3812–3817
17. Bunk, D. M. (1997) *Anal. Chem.* **69,** 2457–2463
18. Wada, Y. (1996) *J. Mass Spectrom.* **31,** 263–266
19. Zhao, H. R., Smith, J. B., Jiang, X. Y., and Abraham, E. C. (1996) *Biochem. Biophys. Res. Commun.* **229,** 128–133
20. Munoz, V., and Serrano, L. (1995) *J. Mol. Biol.* **245,** 275–296
21. Munoz, V., and Serrano, L. (1994) *Nat. Struct. Biol.* **1,** 399–409
22. Delaglio, F., Grzesiek, S., Vuister, G. W., Zhu, G., Pfeifer, J., and Bax, A. (1995) *J. Biomol. NMR* **6,** 277–293
23. Johnson, B. A., and Blevins, R. A. (1994) *J. Biomol. NMR* **4,** 603–614
24. Brunger, A. T., Adams, P. D., Clore, G. M., DeLano, W. L., Gros, P., Grosse-Kunstleve, R. W., Jiang, J. S., Kuszewski, J., Nilges, M., Pannu, N. S., Read, R. J., Rice, L. M., Simonson, T., and Warren, G. L. (1998) *Acta Crystallogr. Sect. D Biol. Crystallogr.* **54,** 905–921
25. Koradi, R., Billeter, M., and Wuthrich, K. (1996) *J. Mol. Graph.* **14,** 51–55
26. Laskowski, R. A., Rullmannn, J. A., MacArthur, M. W., Kaptein, R., and Thornton, J. M. (1996) *J. Biomol. NMR* **8,** 477–486
27. van Gunsteren, W. F., Brunne, R. M., Gros, P., van Schaik, R. C., Schiffer, C. A., and Torda, A. E. (1994) *Methods Enzymol.* **239,** 619–654
28. Guex, N., and Peitsch, M. C. (1997) *Electrophoresis* **18,** 2714–2723

29. Rohovec, J., Maschmeyer, T., Aime, S., and Peters, J. A. (2003) *Chemistry* **9,** 2193–2199
30. Cavanagh, J., Fairbrother, W. J., Palmer, A. G., and Skelton, N. J. (1996) *Protein NMR Spectroscopy: Principles and Practice*, Academic Press, Orlando, FL
31. Smales, C. M., Pepper, D. S., and James, D. C. (2000) *Biotechnol. Bioeng.* **67,** 177–188
32. Wishart, D. S., and Sykes, B. D. (1994) *Methods Enzymol.* **239,** 363–392
33. Wuthrich, K. (1986) *NMR of Proteins and Nucleic Acids*, Wiley Interscience, New York
34. Williamson, R. A., Muskett, F. W., Howard, M. J., Freedman, R. B., and Carr, M. D. (1999) *J. Biol. Chem.* **274,** 37226–37232
35. Arumugam, S., Gao, G., Patton, B. L., Semenchenko, V., Brew, K., and Van Doren, S. R. (2003) *J. Mol. Biol.* **327,** 719–734
36. Coussons, P. J., Jacoby, J., McKay, A., Kelly, S. M., Price, N. C., and Hunt, J. V. (1997) *Free Radic. Biol. Med.* **22,** 1217–1227
37. Ahmed, N., Dobler, D., Dean, M., and Thornalley, P. J. (2005) *J. Biol. Chem.* **280,** 5724–5732